AD-A133 806 INJECTION ATOMIZATION IGNITION AND COMBUSTION OF LIQUID 1/1
FUELS IN HIGH-SPE..(U) VIRGINIA POLYTECHNIC INST AND
STATE UNIV BLACKSBURG DEPT OFAA.. J A SCHETZ JAN 83
UNCLASSIFIED VPI-AERO-131 AFOSR-TR-83-0864 AFOSR-82-0159 F/G 21/2 NL

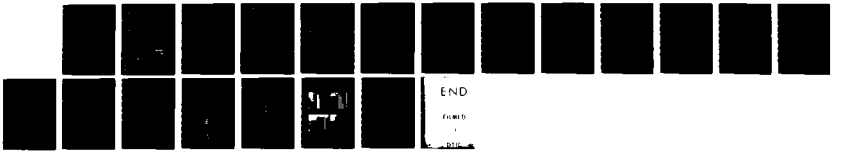

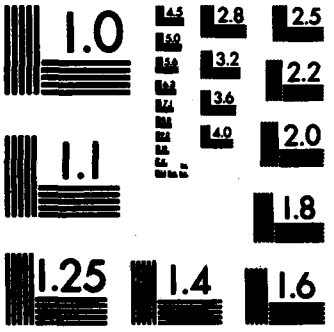

COLLEGE OF ENGINEERING

AFOSR Annual Scientific Report
Grant AFOSR 82-0159

Jan. 1983
VPI-Aero-131

INJECTION, ATOMIZATION, IGNITION AND COMBUSTION OF LIQUID FUELS IN HIGH-SPEED AIR STREAMS

Joseph A. Schetz

Aerospace and Ocean Engineering Department

VIRGINIA POLYTECHNIC INSTITUTE AND STATE UNIVERSITY

BLACKSBURG, VIRGINIA

AFOSR Annual Scientific Report
Grant AFOSR 82-0159

Jan. 1983
VPI-Aero-131

INJECTION, ATOMIZATION, IGNITION AND COMBUSTION OF LIQUID FUELS IN HIGH-SPEED AIR STREAMS

Joseph A. Schetz

Aerospace and Ocean Engineering Department

UNCLASSIFIED
SECURITY CLASSIFICATION OF THIS PAGE (When Data Entered)

REPORT DOCUMENTATION PAGE		READ INSTRUCTIONS BEFORE COMPLETING FORM
1. REPORT NUMBER AFOSR-TR- 83-0864	2. GOVT ACCESSION NO.	3. RECIPIENT'S CATALOG NUMBER
4. TITLE (and Subtitle) INJECTION, ATOMIZATION, IGNITION AND COMBUSTION OF LIQUID FUELS IN HIGH-SPEED AIR STREAMS		5. TYPE OF REPORT & PERIOD COVERED ANNUAL: 01 DEC 81-31 DEC 82
		6. PERFORMING ORG. REPORT NUMBER VPI-Aero-131
7. AUTHOR(s) J A Schetz		8. CONTRACT OR GRANT NUMBER(s) AFOSR-82-0159
9. PERFORMING ORGANIZATION NAME AND ADDRESS Virginia Polytechnic Institute and State Univ. Aerospace and Ocean Engineering Department Blacksburg, VA 24061		10. PROGRAM ELEMENT, PROJECT, TASK AREA & WORK UNIT NUMBERS 61102F 2308/A2
11. CONTROLLING OFFICE NAME AND ADDRESS Air Force Office of Scientific Research/NA Bldg. 410 Bolling Air Force Base, D. C. 20332		12. REPORT DATE Jan 1983
		13. NUMBER OF PAGES
14. MONITORING AGENCY NAME & ADDRESS(if different from Controlling Office)		15. SECURITY CLASS. (of this report) Unclassified
		15a. DECLASSIFICATION/DOWNGRADING SCHEDULE

16. DISTRIBUTION STATEMENT (of this Report)

Approved for Public Release; distribution unlimited

17. DISTRIBUTION STATEMENT (of the abstract entered in Block 20, if different from Report)

18. SUPPLEMENTARY NOTES

19. KEY WORDS (Continue on reverse side if necessary and identify by block number)

Transverse Injection, Simulation, Fuel Injection, Spray Plume, Droplets

20. ABSTRACT (Continue on reverse side if necessary and identify by block number)

A simulation approach to studying hot flow subsonic cross-stream fuel injection problems in a less complex and costly cold flow facility was developed and implemented. A typical ramjet combustion chamber fuel injection problem was posed where ambient temperature fuel (Kerosene) is injected into a hot airstream. This case was transformed through two new similarity parameters involving injection and freestream properties to a simulated case where a chilled injectant is injected into an ambient temperature airstream. →

DD FORM 1 JAN 73 1473 EDITION OF 1 NOV 65 IS OBSOLETE

UNCLASSIFIED
SECURITY CLASSIFICATION OF THIS PAGE (When Data Entered)

20. (cont'd)

Experiments for the simulated case using chilled Freon-12 injected into the Virginia Tech 23 x 23 cm. blow-down wind tunnel at a freestream Mach number of 0.44 were run. The freestream stagnation pressure and temperature were held at 2.5 atm. and 300°K respectively. The results showed a clear picture of the mechanisms of jet decomposition in the presence of rapid vaporization. Immediately after injection a vapor cloud was formed in the jet plume, which dissipated downstream leaving droplets on the order of 8 to 10 microns in diameter for the conditions examined. This represents a substantial reduction compared to baseline tests run at the same conditions with water which had little vaporization. The desirability of using slurry fuels for aerospace application has long been recognized, but the problems of slurry combustion have delayed their use. The present work is an experimental and numerical investigation into the break-up and droplet formation of laminar slurry jets issuing into quiescent air. A nozzle with a 0.74mm diameter orifice was vibrated in the axial direction with an electro-mechanical vibrator. The slurry chosen was a water liquid phase with glass beads of 3-37 microns in diameter for the solid phase. The velocity of the jet was varied between 0.5 and 3 meters per second and the disturbance length was varied between 3 and 6 jet diameters. Mass loadings of from 10 to 50 percent were investigated. The growth due to capillary forces of the disturbances was measured from photographs. A numerical code for solving the Navier-Stokes equations was modified by the addition of equations simulating particles in the flowfield. Experimentally and numerically, it was found that a simple, gross variable such as the growth rate between the peaks and troughs of the slurry could be predicted by extensions of the linear theory of Lord Rayleigh. It was found, however, that the presence of particles in the jet caused changes in the detailed shape of the jet. Break-up of the jet became irregular when particles were introduced. In some cases, alternate disturbances showed different growth rates on the slurry jets causing formation of much larger drops than were formed by the liquid jet. The numerical analysis predicted larger satellite drops than were found experimentally. In general, the break-up of slurries is less predictable and more sensitive to external disturbance than the liquid jet.

Research Objectives

Interest in the ramjet/scramjet field due to the potential performance benefits for missile, projectile and aircraft propulsion continues to be strong. The complex physical and chemical processes resulting from transverse injection of liquid and/or liquid-slurry fuel jets into high speed airstreams find direct application in these and several other propulsion-related systems. For supersonic airstreams, these include thrust vector control and external burning in the wake region of projectiles, as well as scramjet engines. For subsonic airstreams, the other applications include "dump" combustors on devices such as integral rocket ramjets, afterburners and dumping of cooling water out the end of turbine blades, in addition to subsonic ramjet devices.

The important phenomena in all of these applications include physical processes associated with gross penetration; jet fracture, breakup and atomization; phase separation and, in some chemical processes associated with ignition and combustion. Studies at Virginia Tech during the subject time period concentrated on various aspects of the complex physical processes involved.

Effects of Physical Properties

The effects of the variation of vapor pressure with temperature of a liquid fuel are very important in describing the rate of fuel evaporation along the jet plume as it is heated by the air stream in the combustor. Studies were undertaken to develop methods of simulating these phenomena

under cold-flow test conditions and to make measurements.

Slurry Jet Break-up

Numerical and experimental studies of the break-up of slurry (particle-laden) jets in air are to be performed to aid in developing a fundamental understanding of the processes involved.

Status of the Research

Effects of Physical Properties

A simulation approach to studying hot flow subsonic cross-stream fuel injection problems in a less complex and costly cold flow facility was developed and implemented. The simulation problem that we wish to address can can be stated as follows. If all the mechanical aspects of the prototype and model injection problems are matched except heating, how can the effects of heating and thus vaporization along the plume be simulated with an ambient temperature air flow? Thus, we will require at least close matches of: injector size and shape, injectant flow rate (expressed as $\bar{q} \equiv \rho_j V_j^2/\rho_\infty V_\infty^2$), crossflow Mach number and injectant density, viscosity and surface tension. This would be enough to insure equivalence if heating were not important. In the prototype case, ambient temperature fuel (e.g. Kerosene) is injected across a hot air stream. At the injection temperature, the vapor pressure is low, and there is little evaporization. As the liquid is heated along the trajectory of the jet, the vapor pressure rises rapidly, and there is substantial evaporization. There is, therefore, some time history of temperature (and vapor pressure) along the plume, and that is the process that we wish to simulate.

To put this all on a rational basis, we must introduce nondimensional expressions involving the vapor pressure and the driving force for heating - the difference between the injection temperature and the air stagnation temperature. The relevant reference point for the local vapor pressure is the static pressure, and this difference can be normalized with the dynamic pressure, so we choose the parameter

$$\sigma(T) \equiv \frac{p_v(T)-p_\infty}{\frac{1}{2}\rho_\infty V_\infty^2}$$

This can be recognized as what is often termed a Cavitation Number in a different context. For a suitable dimensionless temperature difference, we choose simply

$$T^* \equiv \frac{T_{0,\infty}-T_j}{T_{0,\infty}}$$

By physical reasoning then, we have developed a simulation procedure that requires matching all the mechanical parameters mentioned earlier and now T* and $\sigma(T_j)$ and $\sigma(T_{0,\infty})$. This latter point is the condition that the liquid jet tends toward as it is heated along the trajectory.

For this investigation, an example case was chosen to demonstrate how these parameters can be used to create a simulation of a real case of fuel injection. Consider a ramjet engine traveling at a freestream Mach number of 2.1 at 60,000 ft. Assuming diffusion to a Mach number of 0.44 in the combustor yields a stagnation temperature of 405°K in the combustor entrance plane and a stagnation pressure of 0.884 atm. Now consider Kerosene fuel injected at 25°C. At this point p_v = 0.033 atm. so,

$$(\sigma_j)_{pro} = -5.7$$

$$(T_j^*)_{pro} = 0.26$$

After injection, but before combustion begins, the fuel will be heated and begin the vaporization process. The maximum value the fuel would be heated to would be the freestream stagnation value of 405°K. At this temperature, the vapor pressure of Kerosene is 2.993 atm., and

$$(\sigma_\infty)_{pro} = 17.6$$

$$(T_\infty^*)_{pro} = 0$$

This establishes the endpoints in the heating process for the hot flow case and the basis for the flow problem to be modelled. The task now becomes transforming the process into one which can be implemented in a cold flow wind tunnel facility.

The wind tunnel freestream Mach number was taken as the same as that in the combustor for the real case, M = 0.44. In establishing a value for stagnation pressure, a compromise must be reached between operable values for the wind tunnel available and the satisfaction of matching requirements. A value of 2.517 atm adequately satisfied these needs, generating the pressure ratios which enter in a later discussion. This value fixes the freestream static and dynamic pressures at 2.204 and 0.313 atm. respectively. The stagnation temperature of the facility was that of ambient air or 25°C. With these figures to work with, a fluid must be found such that the values

of σ and T* are matched with the real case at injection and at tunnel stagnation conditions.

At injection, the value of $(T^*)_{sim}$ must be 0.26. Since the wind tunnel stagnation temperature is known, this fixed the injection temperature at -50°C. Therefore, a model fluid had to be found with a vapor pressure of 0.422 atm. at -50°C in order to match the conditions at injection $(\sigma_j)_{sim} = (\sigma_j)_{pro} = -5.7$. Freon-12 is found to have a vapor pressure of 0.388 atm. at -50°C. Additionally, the model fluid must have a vapor pressure of 7.483 atm. at 25°C in order to match end point conditions $(\sigma_\infty)_{sim} = (\sigma_\infty)_{pro} = 17.6$. Freon-12 is found to have a vapor pressure of 6.802 atm at 25°C. The physical property values and density are also a reasonable match with Kerosene. The similarity parameters are summarized as follows:

Kerosene Prototype (Hot Flow) Case	Freon-12 Simulated (Cold Flow) Case
$T_j = 25°C$	$T_j = -50°C$
$T_o = 132°C$	$T_o = 25°C$
$\sigma_j = -5.7$	$\sigma_j = -5.8$
$\sigma_\infty = 17.6$	$\sigma_\infty = 15.0$
$T_j^* = .26$	$T_j^* = .26$
$T_\infty^* = 0$	$T_\infty^* = 0$
Viscosity @ $T_j = 0.19$ centipoise	Viscosity @ $T_j = 0.26$ centipoise
Specific gravity = 0.8	Specific gravity = 1.3

Surface tension @ T_j =
[illegible] dyne/cm

Heat of vaporization =
[illegible] cal/gm

Surface tension @ T_j =
19 dyne/cm

Heat of vaporization =
39.5 cal/gram

The first tests produced spark photographs of Freon-12 injected at [illegible] The photographs were arranged in order of increasing injectant [illegible] (i.e. less "chilling" starting from the -50°C simulated point). The first observation was the "cloud-like" appearance of the plume. This [illegible] case where the distinct formation of individual drop- [illegible] clearly seen. It is possible, however, to view larger droplets in [illegible] the cloud is less dense. The process of initial jet decomposition [illegible] of the injectant, but a mechanism similar to [illegible] heating and evaporation of the injectant along [illegible] the fog-like appearance of the jet plume. As the [illegible] increases, it was seen that the fog is [illegible]

[illegible] the streak photographs was the penetration of [illegible] downstream. For each case in the test matrix, a streak [illegible] and the data was used to determine a judicious place- [illegible] sampling. Additionally, the penetration was [illegible] of 20 diameters downstream of the injector for each [illegible] results are plotted as non-dimensional penetration (h/d_j) [illegible]). As can be seen, there is a small reduction in [illegible] range of conditions compared to non-evaporating water

injection.

The next step in the investigation was to obtain a droplet size distribution for the cases studied. The results of these measurements are shown in Fig. No. 2 for the case of water at $\bar{q} = 1$ and 4. The $\bar{X}$ and y/h axes locate the space coordinates along the plume and mean droplet diameters are plotted along the normal axis. These results show that for injection at $\bar{q} = 4$ the larger droplets initially occupy a region close to the upper edge of the plume. As they are carried downstream they become more evenly distributed along the plume centerline and then gradually settle closer to the injection plane. It should also be noted that the droplet diameters are decreasing in the downstream direction as further atomization and evaporation take place.

The results for water injected at $\bar{q} = 1$ show slightly different droplet distribution. At all stations considered, the larger droplets remained in the lower portion of the jet plume. Again, as the droplets travel downstream the mean droplet diameters decrease. It can also be observed that at virtually all stations, the droplets are larger for the lower injection rate. The results can be generalized as follows: 1) by increasing $\bar{q}$, which is proportional to the jet velocity squared, the degree of atomization is increased, and smaller droplets result, 2) as the downstream distance from the injector increases, the mean droplet diameter decreases, and 3) the larger droplets eventually migrate to the lower portion of the plume for the case of a higher dynamic pressure ratio, whereas for a lower $\bar{q}$, the larger droplets are always found close to the wall.

As was previously mentioned from the spark shadowgraphs, a cloud of very small droplets surrounds the jet plume when the readily evaporated Freon-12

is injected. This cloud presents problems for the droplet size measurements because the method is based on the scattering of light and the cloud presents problems because of increased absorption of the laser beam and multiple scattering. It was found, however, that measurements could be made farther downstream after some of the cloud had evaporated. The results from Freon-12 injected at $\bar{q} = 4$ and $T_j = -10, -30, -50°C$ are shown in Fig. No. 3. Upon examining the data for the model case, ($T_j = -50°C$, $\sigma_j = -5.8$, $T_j^* = .26$) with $\bar{q} = 4$ it can be seen that the profile of the droplet sizes is similar to water with the larger droplets lower in the plume. However, the droplet diameters have been reduced an average of 55% from the water case. By raising the injection temperature to -30°C, σ is increased by 33% and T* is decreased T* by 27%, thereby increasing the rate of evaporation. In doing this, the average droplet diameter at this station drops 10% over the model case. By increasing the injection temperature even further to -10°C, T* is decreased an additional 27% and σ is increased to 0.16 where the Freon is injected as a nearly saturated liquid. For this case, the average droplet size is decreased an additional 6%.

This work is reported in detail in AIAA Paper No. 83-0419.

Slurry Jet Injection

The desirability of using slurry fuels for aerospace application has long been recognized, but the problems of slurry combustion have delayed their use. The present work is an experimental and numerical investigation into the break-up and subsequent droplet formation of laminar slurry jets issuing into quiescent air. A nozzle with a 0.74 mm diameter orifice was

vibrated in the axial direction with an electro-mechanical vibrator. The vibrations regulated the break-up of the jet issuing from the nozzle. For the experiments the slurry chosen was a water liquid phase with glass beads of 3-37 microns in diameter for the solid phase. The velocity of the jet was varied between 0.5 and 3 meters per second and the disturbance length was varied between 3 and 6 jet diameters. Mass loadings of from 10 to 50 percent were investigated. The growth due to capillary forces of the disturbances was measured from photographs. A numerical code for solving the Navier-Stokes equations developed by Los Alamos Scientific Laboratories was modified by the addition of equations simulating particles in the flowfield. This modified code was employed to calculate the velocity distribution, the pressure distribution and the shape of slurry jets under the action of surface tension. Experimentally and numerically, it was found that a simple, gross variable such as the growth rate between the peaks and troughs of the slurry could be predicted by extensions of the linear theory of Lord Rayleigh. It was found, however, that the presence of particles in the jet caused changes in the detailed shape of the jet. Break-up of the jet became irregular when particles were introduced. In some cases, alternate disturbances showed different growth rates on the slurry jets causing formation of much larger drops than were formed by the liquid jet. The numerical analysis predicted larger satelliite drops than were found experimentally. In general, the break-up of slurries is less predictable and more sensitive to external disturbance than the liquid jet.

The all-liquid jet broke up into regular droplets. Typical results for this may be seen in Fig. No. 4. The effect of large amplitude initial disturbance and the nearness of the jet (60 mm upstream) are apparent in this figure. The wavelength of the disturbance is about 4.6 diameters.

Under the same test conditions, regular stable break-up of the slurry was extremely difficult to achieve. Results of experiments with slurries are shown in Fig. Nos. 5 through 7. Figure 5 is a back-lighted photograph of a slurry jet with a disturbance wavelength of 3.85 diameters and a mass loading of 14 percent. In each of the photographs, the jet is directed vertically downward, the scale on the left is in centimeters and the dark objects near the center of Fig. Nos. 4, 6 and 7 are cylindrical wires of 0.711, 0.742, and 0.787 mm diameter. Though in these photographs the growth of the waves is fairly regular, lack of symmetry is apparent. The slurry jet, for all conditions tested, is not as stable as the liquid jet and will not readily break into uniform equally spaced droplets.

The negatives for the photographs of the experiments were placed in a precise optical comparator. The swells and necks of the jet disturbances were measured to 0.02 mm accuracy. The time between successive disturbances was calculated from the known frequency of the initial disturbance. Non-dimensionalized graphs of the results of four of these photographs are shown in Figure 8 through 11. The "inner" data points refer to the growth of the necks, the "outer" data points refer to the swells and the solid line is a least squares fit through the data points. The graphs in Figures 8 through 11 are taken from the data shown in Figures 4 through 7. By comparing Figure 8 to Figures 9, 10 and 11, the increase in irregularity and data scatter which is always present in the slurry is apparent.

This work is still in progress. The results obtained to date are described in AIAA Paper No. 83-0067.

Professional Personnel

Dr. Joseph A. Schetz

Interactions

Various groups in government, universities and industry continue to use our results published in the open literature for design and to support further research. In 1982, we have also been contacted directly by engineers from the Atlantic Research Corp., Southwest Research Inst., NASA Langley Research Center, Applied Physics Lab., and Carnegie-Mellon and Princeton Universities.

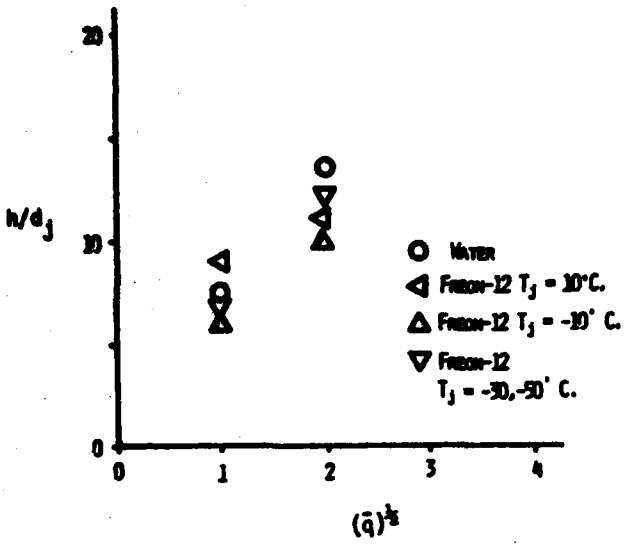

Fig. 1 Penetration Plot of Various Injectants

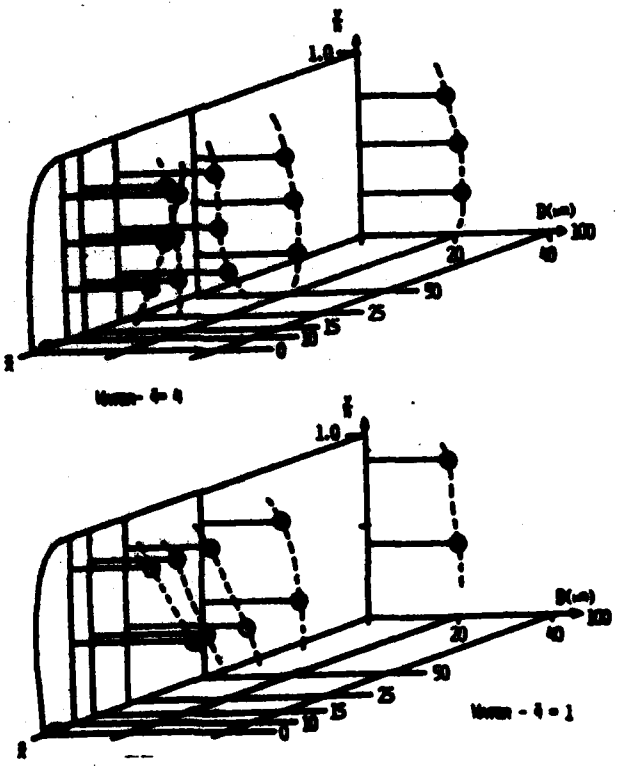

Fig 2 Droplet Distribution in Plume Water - $\bar{q}$ = 1 and 4.

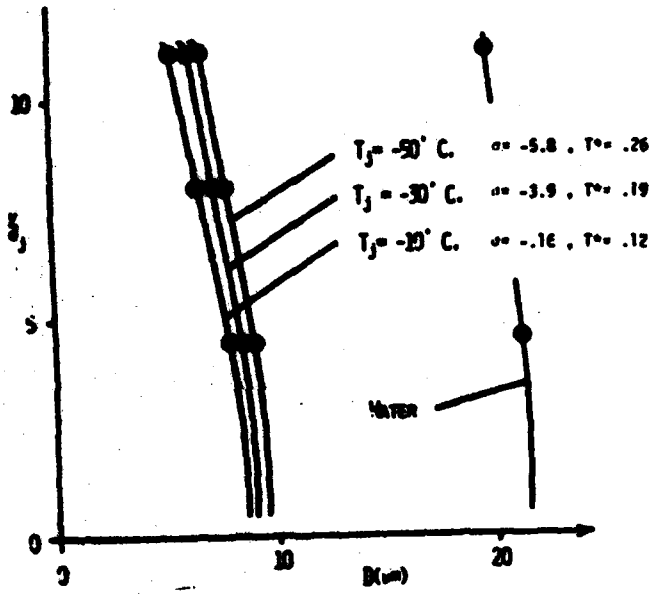

Fig. 3 Droplet Profile at $\bar{x}$ = 100
Freon-12, $\bar{q}$ = 4

Fig. No. 4 Photograph of Jet Break - up
x/D = 4.65, 0% Loading

Fig. No. 5 Photograph of Jet Break - up
x/D = 4.41, 16% Loading

Fig. No. 6 Photograph of Jet Break - up
x/D = 3.85, 14% Loading

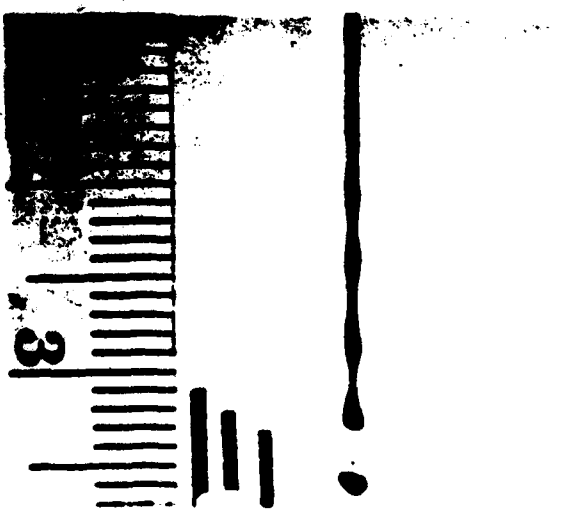

Fig. No. 7 Photograph of Jet Break -up
x/D = 3.83, 17% Loading

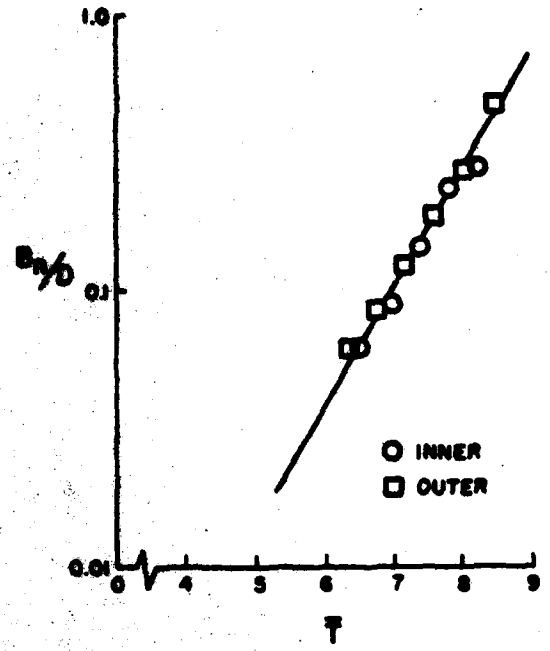

Fig. No. 8 Growth Rate of Disturbances from Experiment: $\lambda/D = 4.65$ 0% Loading

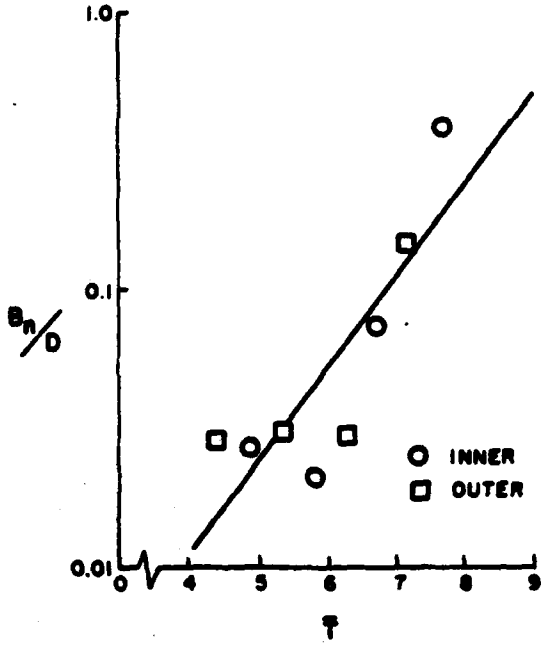

Fig. No. 9 Growth Rate of Disturbances from Experiment: $\lambda/D = 4.41$ 16% Loading

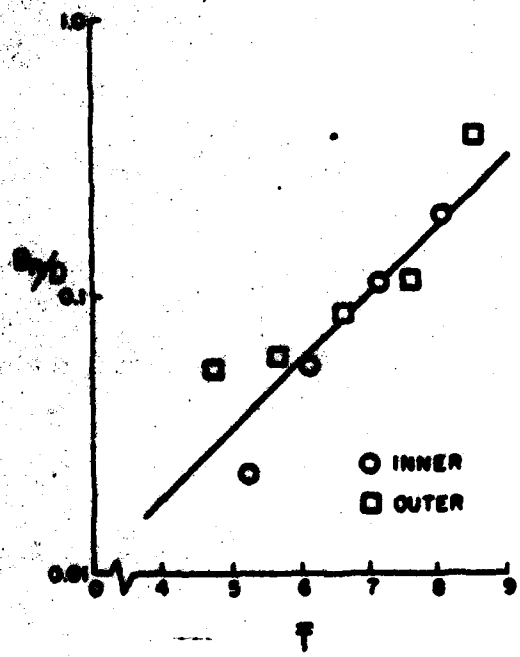

Fig. No. 10 Growth Rate of Disturbances from Experiment: $\lambda/D = 3.86$ 14% Loading

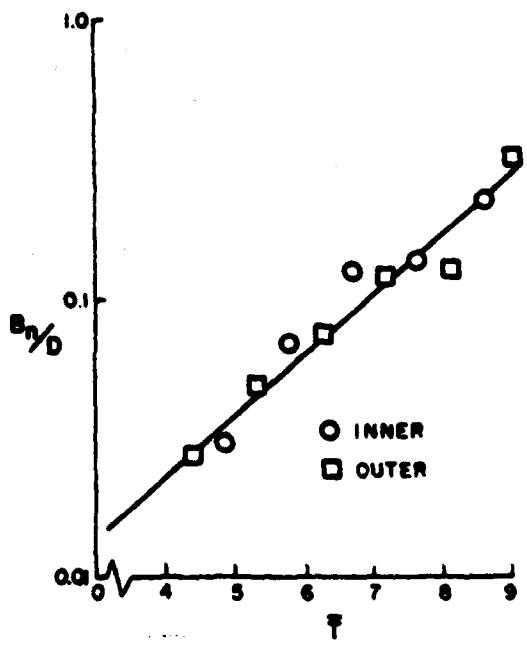

Fig. No. 11 Growth Rate of Disturbances from Experiment: $\lambda/D = 3.83$ 17% Loading

END

FILMED

11-83

DTIC